GEOPHYSICAL RESEARCH LETTERS, VOL. 28, NO. 19, PAGES 3665-3668, OCTOBER 1, 2001

Ultraviolet radiation in partly snow covered terrain: Observations and three-dimensional simulations

Arve Kylling[1] and Bernhard Mayer[2]

Abstract. Coastal regions with fiords and mountains with seasonally varying snowcover form complex environments for ultraviolet radiative transfer. The presence of snow causes enhanced levels of UV radiation, the quantitative interpretation of which is only possible with detailed three-dimensional radiative transfer simulations. Such calculations of the irradiance at 340 nm have been performed for the location of Tromsø, Norway, under cloudless and overcast conditions, moving the snowline from 0 to 1000 m.a.s.l. and finally for snow free conditions. The evolution of the radiation enhancement as the snowline moves up is compared with measurements made by a narrow bandwidth multichannel filter instrument. For a cloudless sky the simulations and measurements exhibit a similar radiation enhancement of 23-27%. For the investigated overcast situation the radiation enhancement is about 40-60%.

Introduction

The Earth's surface forms a complex lower boundary for atmospheric radiative transfer. Its optical properties are highly inhomogeneous and vary with altitude and season. To realistically quantify the influence of surface albedo on radiation poses a challenging problem for both experimentalists and modellers.

Degünther et al. [1998], *Degünther and Meerkötter* [2000], and *Lenoble* [2000] performed three-dimensional (3D) radiative transfer calculations for various idealized snow distributions under cloudless and overcast conditions. They found that the ultraviolet (UV) irradiance may be influenced by albedo variations more than 10 – 20 km away. The presence of clouds increased the albedo effect on the surface UV irradiance but at the same time decreased the area of importance. These general results agreed with the site specific studies performed for Palmer Station [*Ricchiazzi and Gautier*, 1998] and McMurdo [*Podgorny and Lubin*, 1998]. *Smolskaia et al.* [1999] experimentally investigated the effect of the stepfunction like behavior of the ocean-snow surface albedo for Davis Station and reported a smaller effect than anticipated. *Mayer and Degünther* [2000] simulated the situation and concluded that the measurements needed to be taken both further offshore and inland to see the full effect.

In this paper the first 3D radiative transfer simulations taking into account the seasonally changing snowline are presented. The simulations are compared with measurements for both cloudless and overcast situations.

[1]Norwegian Institute for Air Research, Kjeller.
[2]Deutsches Zentrum für Luft- und Raumfahrt (DLR), Germany.

Paper number 2001GL013034.
0094-8276/01/2001GL013034$05.00

Theory

For a nonzero surface albedo a fraction of the downwelling radiation will be reflected upwards. Part of the reflected radiation will be scattered downward again increasing the global downwelling irradiance at the surface compared to a surface with zero albedo. For the case of Lambertian reflection, the magnitude of this increase can be quantified starting from the downwelling global irradiance for zero albedo, $E(\Lambda = 0)$. For a nonzero albedo, a fraction $\Lambda(x, y)$ of $E(\Lambda = 0)$ is reflected upward by the surface from the point (x, y). A certain fraction of this upwelling, isotropic irradiance is scattered back to the surface by the overlying atmosphere. Due to this process, the irradiance is increased by

$$E^{(1)}(x, y) = \int \Lambda(x', y') E^{(0)}(x', y') s(\rho) dS' \qquad (1)$$

where $E^{(0)}(x, y) = E(\Lambda = 0, x, y)$ is the irradiance for zero surface albedo, $\rho = \sqrt{(x - x')^2 + (y - y')^2}$ is the distance between the points (x, y) and (x', y'), and $s(\rho)dS'$ is the probability that a photon reflected inside an area element dS' around (x', y') will hit the surface at (x, y), after being scattered downwards by the atmosphere which is assumed to be horizontally homogeneous for this purpose. A part of $E^{(1)}$ is reflected again, leading to an iterative process which quickly converges towards zero:

$$E^{(i+1)}(x, y) = \int \Lambda(x', y') E^{(i)}(x', y') s(\rho) dS' \qquad (2)$$

The total surface irradiance $E(x, y)$ is finally the sum of all contributions

$$E(x, y) = \sum_{i=0}^{\infty} E^{(i)} \qquad (3)$$

Evaluating $s(\rho)$ with a Monte Carlo model, $E(x, y)$ can and has been successfully calculated with only few iterations of (2). If neither the atmospheric nor the surface properties vary with x and y, (2) and (3) are reduced to a simple geometric series [*Kylling et al.*, 2000b]. If effects of a non-Lambertian surface reflectance, a horizontally inhomogeneous atmosphere, or topography are to be considered, only a real 3D model can provide a solution.

Simulations

The enhancement of UV radiation due to the presence of snow depends on the fraction of the surface area covered by snow and by its spatial distribution. A complex example is the location of Tromsø, Norway (69.65° N, 18.95° E). The surroundings of Tromsø form a mixture of surfaces with open fiords surrounded by high mountains [*Kylling et al.*, 2000b]. Snow is persistent into early summer and UV measurements are available against which the model simulations will be compared below. Figure 1 shows the area covered

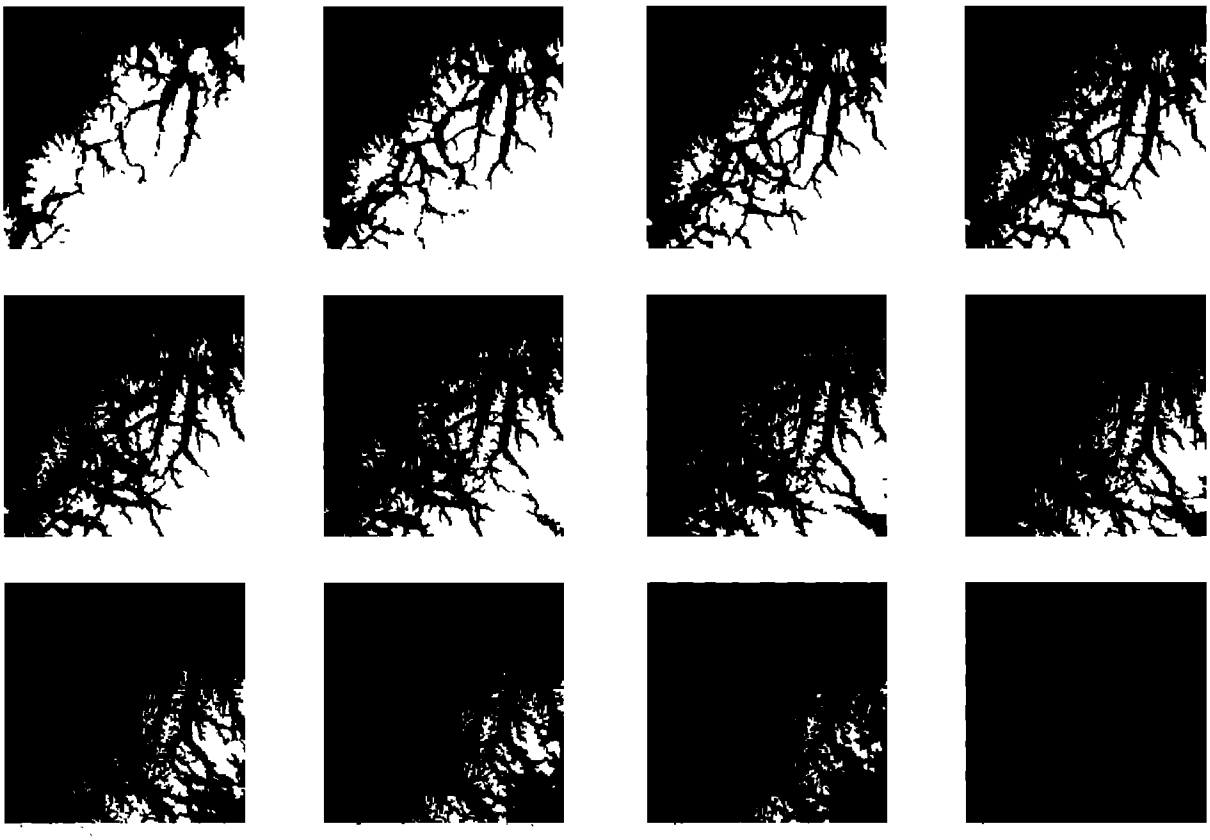

Figure 1. The snow covered and snow free areas surrounding Tromsø (center of frames), Norway, when moving the snowline from 0 m.a.s.l. (top left) to 1000 m.a.s.l. (bottom, second from the right) in steps of 100 m. Snow free areas are painted black and snow covered areas are shown in white. In the top left frame black is identical to the ocean and white is land. The bottom right frame illustrates snow free conditions. The domain size is 201×201 km^2.

by snow (white) as a function of the snowline which starts at 0 m.a.s.l. (upper left) to 1000 m.a.s.l. (bottom second from right), in steps of 100 m. The ocean and fiords are assumed to be ice free which is in general true for all but the innermost parts of the largest fiords within the domain.

The three-dimensional radiative transfer simulations were performed with MYSTIC (Monte Carlo code for the physically correct tracing of photons in cloudy atmospheres), see e.g. [*Kylling et al.*, 2000b] for a short overview. The model domain was 201×201 km^2 with a resolution of 1 km, centered around Tromsø. Elevation information was taken from the GTOPO30 data set (Global 30 Arc Second Elevation data set, available at http://edcwww.cr.usgs.gov/landdaac/gtopo30/gtopo30.html) and regridded to 1×1 km^2 resolution using the Generic Mapping Tools (GMT) [*Wessel and Smith*, 1995]. Between these data points, the surface is interpolated bilinearely by the model to calculate the appropriate surface elevation and inclination at any location. For the simulations a Lambertian albedo of 0.07 is used for the snow free areas including the ocean and an albedo of 0.8 for the snow covered areas. *Kylling et al.*, [2000b] found this combination of albedos able to reproduce the effective albedo measured for the site of Tromsø under cloudless skies. As *Degünther and Meerkötter* [2000] showed, the influence of a non-Lambertion surface reflectance on down-welling UV irradiance is small enough to be neglected for our study. The simulations are performed for a solar zenith angle of 60° with the sun in the South (note that for a flat Lambertian surface the result would not depend on solar zenith angle). The subarctic winter atmosphere model of *Anderson et al.*, [1986] was used with the total ozone column scaled to 340 DU. No aerosols were included. For the overcast simulations a homogeneous cloud located between 2–3 km was introduced. The optical depth of the cloud is 10, the asymmetry factor 0.85 and the single scattering albedo 1.0. A Henyey–Greenstein phase function is assumed. A total of 10^9 photons were traced for each case to give a random error of less than 1% in the presented results.

For the island of Tromsø, the ratio of the downwelling global (direct + diffuse) to the global irradiance for snow free conditions as a function of snowline is shown in Figure 2. Plane–parallel radiative transfer simulations with an albedo of 0.8 give a cloudless sky radiation enhancement in erythemal weighted irradiance of 1.4 compared to the snow-free case (albedo 0.07). The reason for the lower enhancement of 1.27 (solid line in Figure 2) is the mixture of snow free and snow covered surfaces and their effect on the downwelling irradiance [*Kylling et al.*, 2000b]. As expected, the enhancement is larger under overcast conditions (dashed line) due to the increased downward reflectivity of the atmosphere.

Measurements

At the Auroral Observatory, Tromsø, Norway, measurements are routinely made by a Ground–based Ultraviolet Radiometer (GUV-541) narrow bandwidth multichannel instrument. The GUV-541 instrument from Biospherical In-

struments Inc., San Diego, measures the UV irradiance in five channels centered at 305, 313, 320, 340, and 380 nm with a bandwidth of approximately 10 nm full width at half maximum (FWHM) and is part of the Norwegian UV monitoring network that was established in 1995. The instrument was calibrated in May 1995 against a SUV–100 UV-Visible Spectroradiometer in San Diego [*Dahlback*, 1996]. The network includes a travelling standard that once a year is shipped to the manufacturer for calibration against a National Institute of Standards and Technology (NIST) traceable lamp as well as against a SUV–100 spectroradiometer. The GUV-541 in Tromsø is compared with the travelling standard once a year and drifts are corrected where neccessary. The instrument reports irradiance values every minute and is in operation year round.

For comparison with the above 3D radiative transfer simulations, cloudless and overcast subsets of the measurement series for the year 1997 were selected. Cloudless time periods were identified by visual examination of the daily variation in the irradiance values. The crosses in Figure 3 are the 340 nm global irradiances for cloudless days relative to the cloudless average days 177-240 which is representative for snow free conditions.

Overcast situations were selected from the dataset presented by *Kylling et al.*, [2000a]. To facilitate comparison with the 3D simulations, irradiance values at 340 nm for which the effective cloud optical depth was 10 ± 1 and the solar zenith angle $60 \pm 1°$, were selected. By effective cloud optical depth is meant the optical depth that when used in a one–dimensional model best reproduces the measurements [*Dahlback*, 1996]. These irradiances are shown in Figure 3 as encircled crosses. Due to the allowed variations in the effective cloud optical depth and the solar zenith angle, and the inherent uncertainty present for overcast situations, the scatter in Figure 3 is larger for the cloudy data points. A clear enhancement in UV radiation is seen with snow on the ground and the enhancement is larger than for a cloudless sky, as predicted by theory.

Discussion and Conclusions

For cloudless sky, simulations (Figure 2) and observations (Figure 3) agree reasonably well. The simulated radiation

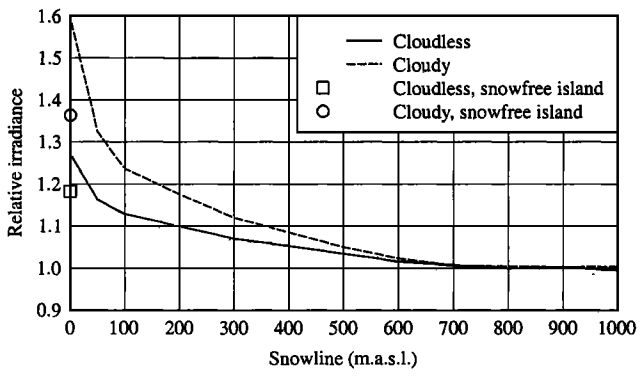

Figure 2. The global irradiance at 340 nm relative to the global irradiance for a snow free domain, as a function of snowline. Cloudless (solid line) and overcast (dashed line) ratios are shown for the island of Tromsø. The □ and ○ are the relative enhancements when the island of Tromsø is snow free, but otherwise all land is snow covered.

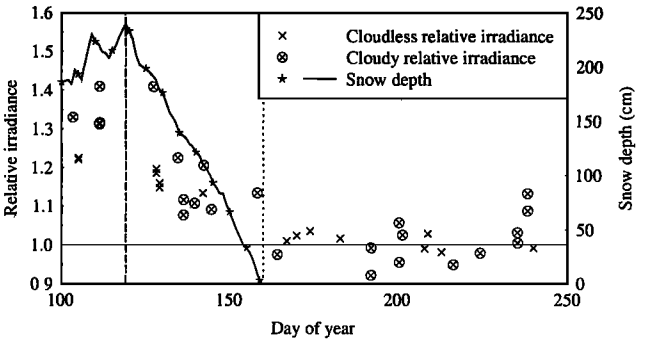

Figure 3. The global irradiance at 340 nm relative to the global irradiance for snow free conditions for the island of Tromsø. The irradiance values are from a GUV-541 instrument for a solar zenith angle of 60°. Days to the left of the dashed vertical line is believed to have a snowline of 0 m.a.s.l. The dotted vertical line indicates the estimated day for when the snowline is 100 m.a.s.l. The snow depth (solid line with stars) is measured at 65 m.a.s.l.

enhancement of 1.27 is slightly larger than the observed maximum, 1.23. With the snowline at 100 m.a.s.l. the simulations predicts 1.13 while the measurements indicate about 1.09. As the snow gradually disappears between days 160–180, the enhancement goes away. The cloudy simulations give a larger enhancement than the cloudless simulations which is in qualitative agreement with the observations (Figure 3). While the simulations predict an enhancement of 1.59 for completely snow covered land, the measurements give a maximum enhancement of 1.42.

Both for the cloudless and the cloudy conditions the simulated radiation enhancements are somewhat larger then the measured ones. A possible explanation for this discrepancy is that for the simulations a single albedo value has been used for all snow covered pixels. The adopted value is representative for clean snow. Pollution, trees, buildings, rocks, and other low albedo surfaces will give a lower value than the one adopted. To test one extreme situation, simulations were performed where all snow was removed from the island of Tromsø while all other land surfaces were snow covered. The enhancement decreases significantly both for cloudless (1.18, square, Figure 2) and overcast (1.36, circle, Figure 2) conditions. Due to the location of the measurement site in the city of Tromsø, a lower albedo value for the pixels close to the measurement site might actually be a better representation of reality. It is also noted that under overcast conditions the surface area of importance is smaller than for a cloudless sky. Thus a too high albedo value for the pixels close to the measurement site results in a larger difference between simulations and measurements for the cloudy than for the cloudless case.

It is noted that the snowline concept is an idealization to some degree. Snowfall over the domain is variable. On the coast snow free conditions often prevail due to the relatively warm ocean and strong winds while snow is abundant inland. Snow vanishes earlier from South facing and wind exposed areas. There is also considerable uncertainty involved in the derivation of the effective cloud optical depth from the GUV-541 measurements. Furthermore, the overcast simulations used a homogeneous cloud, while the real clouds most likely exhibited significant horizontal inhomogeneities. Considering all the uncertainties associated with

the measurements and the albedo and cloud input to the radiation model, the simulations describes the measurements quite well. Both the measured and simulated radiation enhancements decay in a similar manner as the snow disappears, and both the simulated and measured overcast enhancements are larger than the cloudless enhancement.

To fully understand the UV radiation environment in regions with complex surface characteristics, 3D radiative transfer simulations are required. Further improvements include methods to determine the effective surface albedo of individuals pixels, and methods to allow more realistic handling of clouds.

Acknowledgments. A.K. acknowledges support from the COZUV project funded by the Norwegian Research Council.

References

Anderson, G., S. Clough, F. Kneizys, J. Chetwynd, and E. Shettle, AFGL atmospheric constituent profiles (0-120 km), *Tech. Rep. AFGL-TR-86-0110*, Air Force Geophys. Lab., Hanscom Air Force Base, Bedford, Mass., 1986.

Dahlback, A., Measurements of biologically effective UV doses, total ozone abundances, and cloud effects with multichannel, moderate bandwidth filter instruments, *Appl. Opt.*, *35*, 6514–6521, 1996.

Degünther, M., R. Meerkötter, A. Albold, and G. Seckmeyer, Case study on the influence of inhomogeneous surface albedo on UV irradiance, *Geophys. Res. Lett.*, *25*, 3587–3590, 1998.

Degünther, M. and R. Meerkötter, Influence of inhomogeneous surface albedo on UV irradiance: effect of a stratus cloud, *J. Geophys. Res.*, *105*, 22755–22761, 2000.

Kylling, A., A. Dahlback, and B. Mayer, The effect of clouds and surface albedo on UV irradiances at a high latitude site, *Geophys. Res. Lett.*, *27*, 1411–1414, 2000a.

Kylling, A., T. Persen, B. Mayer, and T. Svenøe, Determination of an effective spectral surface albedo from ground based global and direct UV irradiance measurements, *J. Geophys. Res.*, *105*, 4949–4959, 2000b.

Lenoble, J., Influence of the environment reflectance on the ultraviolet zenith radiance for cloudless sky, *Appl. Opt.*, *39*, 4247–4254, 2000.

Mayer, B., and M. Degünther, Comment on "Measurements of erythemal irradiance near Davis Station, Antarctica: Effect of inhomogeneous surface albedo", *Geophys. Res. Lett.*, *27*, 3489–3490, 2000.

Podgorny, I., and D. Lubin, Biologically active insolation over Antarctic waters: Effect of a highly reflecting coastline, *J. Geophys. Res.*, *103*, 2919–2928, 1998.

Ricchiazzi, P., and C. Gautier, Investigation of the effect of surface heterogeneity and topography on the radiation environment of Palmer Station, Antarctica, with a hybrid 3–D radiative transfer model, *J. Geophys. Res.*, *103*, 6161–6176, 1998.

Smolskaia, I., M. Nunez, and K. Michael, Measurements of erythemal irradiance near Davis Station, Antarctic: Effect of inhomogeneous surface albedo, *Geophys. Res. Lett.*, *26*, 1381–1384, 1999.

Wessel, P., and W. H. F. Smith, New version of the Generic Mapping Tools released, *EOS Trans. AGU*, *76–(33)*, 329, 1995.

Arve Kylling, NILU–Kjeller, P.O. Box 100, N-2027 Kjeller, Norway. (arve.kylling@nilu.no)

Bernhard Mayer, Deutsches Zentrum für Luft- und Raumfahrt, Oberpfaffenhofen, D-82234 Weßling, Germany. (bernhard.mayer@dlr.de)

(Received February 15, 2001; revised June 19, 2001; accepted July 6, 2001.)